



# Preparation and characterization of $\text{CoFe}_2\text{O}_4$ powders and films via the sol–gel method

Min Shi\*, Ruzhong Zuo, Yudong Xu, Yunzhi Jiang, Guiyang Yu, Hailin Su, Jiagang Zhong

School of Materials Science and Engineering, Hefei University of Technology, Hefei, Anhui 230009, People's Republic of China

## ARTICLE INFO

### Article history:

Received 11 August 2011  
Received in revised form  
15 September 2011  
Accepted 19 September 2011  
Available online 24 September 2011

### Keywords:

Sol–gel method  
CFO film  
Secondary phases  
Magnetic properties

## ABSTRACT

The  $\text{CoFe}_2\text{O}_4$  (CFO) starting precursor solutions were prepared by two sol–gel methods. The XRD results show that the second sol–gel method is a better method to obtain CFO materials with high purity. The CFO precursor solutions prepared by the second sol–gel method were spin-coated onto the Pt/Ti/SiO<sub>2</sub>/Si substrate to obtain CFO films. With the increase of annealing temperature, the relative amounts of secondary phases in CFO films are decreased. When annealed at 700 °C, CFO films are almost composed of the main phase and the substrate phase without secondary phases. The CFO film is crack-free and has compact structure without any pore. The thickness of CFO film is about 49 nm. The starting precursor solution with the concentration of 0.15 mol L<sup>-1</sup> is better for preparing CFO films. The CFO films with nano-scaled film thicknesses have better magnetic properties than the CFO powders.

© 2011 Elsevier B.V. All rights reserved.

## 1. Introduction

$\text{CoFe}_2\text{O}_4$  (CFO) is a ferrimagnetic spinel oxide structure with high magnetic anisotropy, high saturation magnetization, high wear resistance and good chemical stability [1–3]. CFO in powder and film form has attracted considerable attention for its fundamental understanding and large scale technological applications such as transformer cores, recording heads, antenna rods, loading coils, memory, microwave devices, catalyst, ferrofluids, magnetic refrigeration, solar energy conversion applications and biomedical sensors [4–7]. The CFO film can also be used as magneto-optical materials. The CFO films were mainly prepared by physical methods such as sputtering [8–11], ion-beam deposition [12] and pulsed laser deposition [13]. These methods require expensive laboratory equipment and high vacuum, critical control over processing condition, high cost and long deposition time. However the sol–gel method is a simple, time-saving, low cost method for preparing nano-sized films [14–16]. This method is easy to control the compositions and thickness of films. It has become an attractive method for preparing films.

In this paper, CFO precursor solutions were prepared via two sol–gel methods by selecting different chelators in order to determine the better preparation method. The CFO precursor solutions prepared by the better preparation method were spin-coated onto the Pt/Ti/SiO<sub>2</sub>/Si substrate. Then, the gel films were annealed to

obtain CFO films. The microstructure, phase constitution and magnetic properties of CFO films were investigated as a function of annealing temperature by using scanning electronic microscopy (SEM), an X-ray diffraction (XRD), and vibrating sample magnetometer (VSM).

## 2. Experimental

### 2.1. Preparation of CFO starting precursor solution

#### 2.1.1. The first sol–gel method

Iron nitrate ( $\text{Fe}(\text{NO}_3)_3 \cdot 9\text{H}_2\text{O}$ ) and cobalt acetate ( $\text{Co}(\text{CH}_3\text{CO}_2)_2 \cdot 4\text{H}_2\text{O}$ ) were used as starting materials. Ethylene glycol monomethyl ether ( $\text{C}_3\text{H}_8\text{O}_2 \cdot 4\text{H}_2\text{O}$ ) was used as chelator. Ethanol ( $\text{C}_2\text{H}_5\text{OH}$ ) was used as solvent. The appropriate portions of iron nitrate, cobalt nitrate were dissolved in ethanol, respectively. Solution of iron nitrate and cobalt nitrate was first mixed together, then added ethylene glycol monomethyl ether into above solution and stirred at 80 °C to form a CFO starting precursor solution. The molecule ratio of Co:Fe:C<sub>3</sub>H<sub>8</sub>O<sub>2</sub> is 1:2:1.5. The starting precursor solution was divided into several parts uniformly. They were successively dried at 120 °C to obtain powders for analysis of differential scanning calorimetry and X-ray diffraction.

#### 2.1.2. The second sol–gel method

Iron nitrate ( $\text{Fe}(\text{NO}_3)_3 \cdot 9\text{H}_2\text{O}$ ) and cobalt acetate ( $\text{Co}(\text{CH}_3\text{CO}_2)_2 \cdot 4\text{H}_2\text{O}$ ) were used as starting materials. Citrate ( $\text{C}_6\text{H}_8\text{O}_7$ ) was used as chelator. Ethanol ( $\text{C}_2\text{H}_5\text{OH}$ ) was used as solvent. The appropriate portions of iron nitrate, cobalt nitrate and citric acid were dissolved in ethanol, respectively. Solution of iron nitrate and cobalt nitrate was first mixed together, then added citric acid solution into above solution and stirred at 80 °C to form a CFO starting precursor solution. The molecule ratio of Co:Fe:C<sub>6</sub>H<sub>8</sub>O<sub>7</sub> is 1:2:3. The starting precursor solution was divided into several parts uniformly. They were successively dried at 120 °C to obtain powders for analysis of differential scanning calorimetry and X-ray diffraction.

\* Corresponding author. Fax: +86 551 2905383.

E-mail address: [mrshimindou@hotmail.com](mailto:mrshimindou@hotmail.com) (M. Shi).

## 2.2. Preparation of $\text{CoFe}_2\text{O}_4$ films

The starting precursor solutions were prepared by the second sol–gel methods. Stoichiometric iron nitrate, cobalt nitrate and citrate were first dissolved in ethanol to form a mixed solution. Then, the ethanol was added to adjust concentration of the solution to  $0.15 \text{ mol L}^{-1}$  or  $0.30 \text{ mol L}^{-1}$  to obtain two precursor solutions. The above precursor solutions were spin-coated on the Pt/Ti/SiO<sub>2</sub>/Si substrate a spinning rate of 3500 rpm for 30 s. In order to obtain CFO films, the gel films were dried at  $150^\circ\text{C}$  for 5 min and annealed at different temperatures for 10 min in air and cooled slowly in the furnace.

## 2.3. Characterization

The thermal effects of the CFO powders were analyzed by differential scanning calorimetry (DSC, NETZSCH 404C) at a heating rate of  $5^\circ\text{C min}^{-1}$  in air. X-ray diffraction (XRD, Rigaku D/max-RB) with  $\text{CuK}\alpha$  radiation was used for phase analysis of the powders and films. Cross-section and surface morphologies of CFO films were observed by using scanning electronic microscopy (SEM, FEI Sirion200). Magnetic behavior of the CFO powders and films was characterized by vibration sample magnetometer (VSM, Riken BHV-55).

## 3. Results and discussion

### 3.1. Characterization of starting precursor solution

The CFO starting precursor solutions were successively dried at  $120^\circ\text{C}$  for 30 min, and then ball milled for 10 h. Thus CFO powders were finally obtained. The DSC curves of CFO powders prepared by two sol–gel methods are illustrated in Figs. 1 and 2, respectively. From Fig. 1, it is seen that, for the first sol–gel method, there is an endothermic peak at about  $400^\circ\text{C}$ , an exothermic peak at about  $670^\circ\text{C}$ . The peak at about  $400^\circ\text{C}$  may be due to the decomposition of nitrates. The peaks at about  $670^\circ\text{C}$  may be attributed to the transformation of some intermediate phases to the main phase (CFO). Therefore the annealing temperatures should be above  $670^\circ\text{C}$  in order to obtain CFO materials without secondary phases.

Fig. 2 shows that, for the second sol–gel method, there are two endothermic peaks at about  $120^\circ\text{C}$  and  $400^\circ\text{C}$ , a strong exothermic peak at  $600^\circ\text{C}$ . The peak at about  $120^\circ\text{C}$  may be due to evaporation of solvent. The peak at about  $400^\circ\text{C}$  may be ascribed to the decomposition of citrate. The strong peak at  $600^\circ\text{C}$  may be attributed to the transformation of some intermediate phases to the main phase (CFO). Therefore the annealing temperatures of precursors should be above  $600^\circ\text{C}$  in order to obtain CFO materials without secondary phases. In order to determine the accurate annealing temperatures, CFO powders were characterized by XRD. Fig. 3 shows XRD patterns of CFO powders prepared by the first sol–gel method, which were then annealed at different temperatures. It illustrates that powders

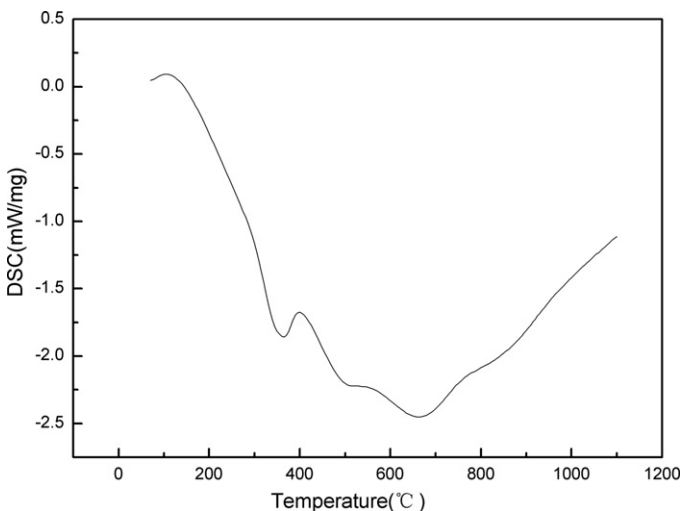


Fig. 1. DSC curve of CFO powders synthesized by the first sol–gel method.

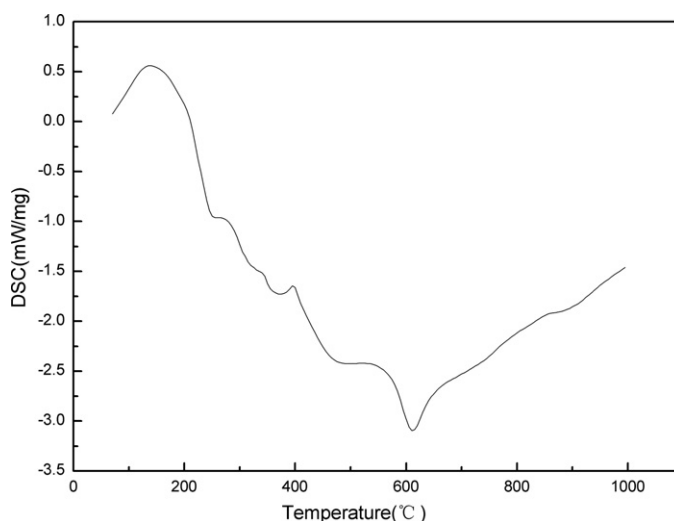


Fig. 2. DSC curve of CFO powders synthesized by the second sol–gel method.

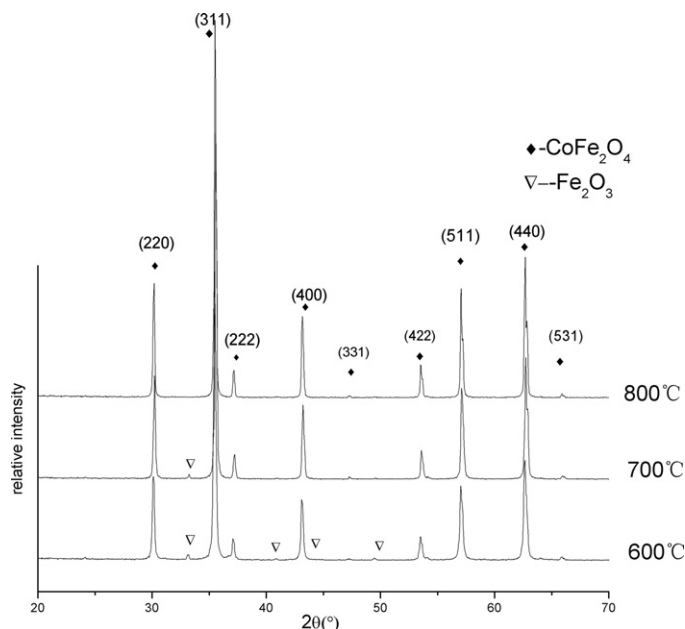


Fig. 3. XRD patterns of CFO powders prepared by the first sol–gel method (annealed at different temperatures for 2 h).

annealed at  $600^\circ\text{C}$  contain a certain amount of secondary phases ( $\text{Fe}_2\text{O}_3$ ) except the main phase ( $\text{CoFe}_2\text{O}_4$ ). With the further increase of the annealing temperature, the fractions of secondary phases decreased remarkably. This shows that the secondary phases have transformed partly to the main phase. Nearly no secondary phases can be detected when the annealing temperature reaches  $800^\circ\text{C}$ . Consequently, the lowest annealing temperature was chosen at  $800^\circ\text{C}$ . The grain sizes of powders prepared by the first sol–gel method and then annealed at different temperatures were calculated by Scherrer's equation using XRD data. The results are shown in Table 1. It is seen that the grain sizes increase with the increase

Table 1

The grain sizes of powders, prepared by the first sol–gel method and then annealed at different temperatures.

Annealing temperature ( $^\circ\text{C}$ )	600	700	800
Grain size (nm)	72	87	99

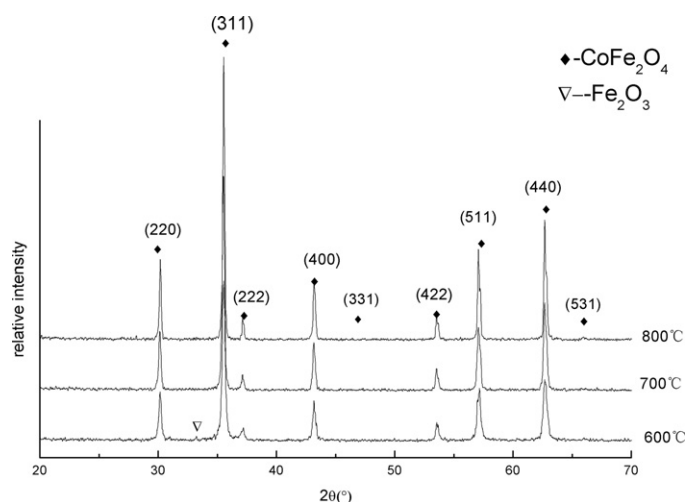


Fig. 4. XRD patterns of CFO powders prepared by the second sol-gel method (annealed at different temperatures for 2 h).

Table 2

The grain sizes of powders, prepared by the second sol-gel method and then annealed at different temperatures.

Annealing temperature (°C)	600	700	800
Grain size (nm)	68	74	85

of annealing temperatures and the grain sizes are smaller than 100 nm.

Fig. 4 shows XRD results of CFO powders prepared by the second sol-gel method, which were then annealed at different temperatures. It is seen that the powders annealed at 600 °C still contain a little amount of secondary phase of Fe<sub>2</sub>O<sub>3</sub> besides the main phase. The relative amount of Fe<sub>2</sub>O<sub>3</sub> is much smaller than that in powders prepared by the first sol-gel method at the same annealing temperature. It is apparent that there is no other detectable impurity phase or secondary phase when the annealing temperature is increased to 700 °C. Therefore the lowest annealing temperature was chosen at 700 °C. On comparing Fig. 4 with Fig. 3, it is apparent that the annealing temperatures of powders prepared by the second sol-gel method are 100 °C lower than those prepared by the first sol-gel method. It can be inferred that the second sol-gel method is a better way to obtain CFO materials with higher purity. The grain sizes of powders prepared by the second sol-gel method and then annealed at different temperatures are listed in Table 2. It also shows that the grain sizes increase with the increase of annealing temperatures. Comparing Table 2 with Table 1, it is seen that, at the same annealing temperature, the grain sizes of powders prepared by the second sol-gel are smaller than those of powders prepared by the first sol-gel method.

Plots of magnetization (M) as a function of applied field (H) for powders prepared by the above-mentioned two sol-gel methods are shown in Fig. 5. It is seen that there exists a typical hysteresis loop. The saturation magnetizations and coercivities of powders, prepared by two sol-gel methods and then annealed at 700 °C, can be drawn from Fig. 5. The results are shown in Table 3. The saturation magnetizations of powders prepared by two sol-gel method

Table 3

The saturation magnetizations and coercivity of powders prepared by two sol-gel methods and then annealed at 700 °C.

Preparation method	Saturation magnetizations (emu g <sup>-1</sup> )	Coercivity (Oe)
The first sol-gel method	78.43	704
The second sol-gel method	82.78	814

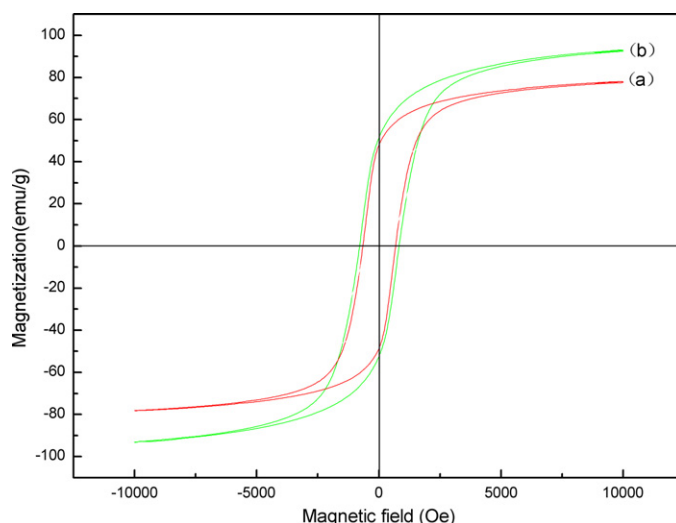


Fig. 5. Hysteresis loops of CFO powders synthesized by different methods, which were then annealed at 700 °C for 2 h: (a) the first sol-gel method and (b) the second sol-gel method.

are both greater than 62 emu g<sup>-1</sup>, reported in reference [17]. It can also be seen that, the coercivity of CFO powders prepared by the second sol-gel method is greater than that of CFO powders prepared by the first sol-gel method. For CFO powders prepared by the first sol-gel method contain more secondary phase which decreases the saturation magnetizations and coercivity, the saturation magnetizations and coercivity of powders prepared by the first sol-gel method are smaller. In short, CFO powders prepared by the second sol-gel method possess greater saturation magnetization and coercivity. They can meet needs of high-density recording media and be candidate for high-density recording media materials [18,19].

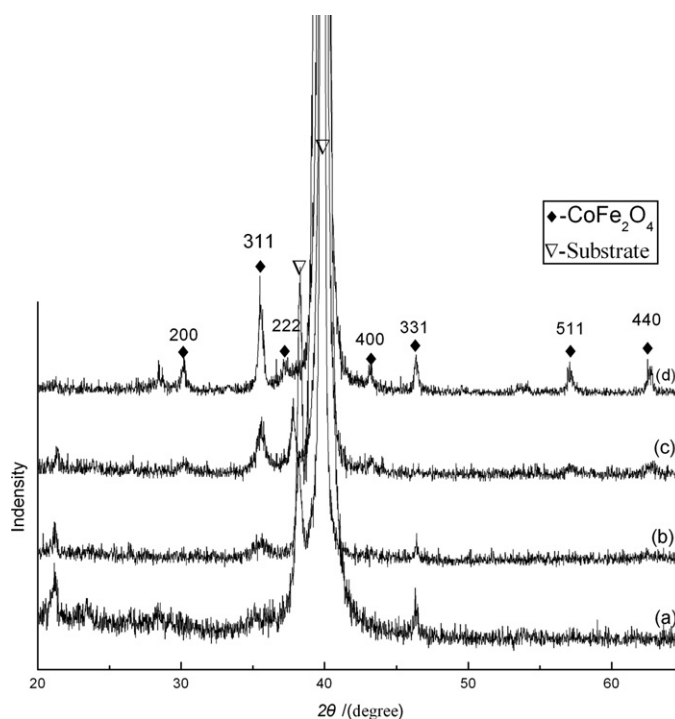


Fig. 6. XRD patterns of CFO films synthesized by the second sol-gel annealed at different temperatures for 10 min. (a) 400 °C; (b) 500 °C; (c) 600 °C; and (d) 700 °C.

In view of purity and magnetism properties, it can be inferred that the second sol–gel method is a better way for preparing CFO materials than the first sol–gel method. Therefore, in this paper, the CFO precursor solutions prepared by the second sol–gel method were spin-coated onto the Pt/Ti/SiO<sub>2</sub>/Si substrate. Then, the gel film was annealed to obtain CFO films.

### 3.2. Characterization of CFO films

Fig. 6 shows XRD patterns of CFO films on the Pt/Ti/SiO<sub>2</sub>/Si substrate via the second sol–gel method, annealed at different temperatures. When annealed at temperature below 600 °C, there are only small amount of main phases (CoFe<sub>2</sub>O<sub>4</sub>) existed in CFO films. When annealed at 700 °C, there are no peaks of secondary phase apart from CFO and substrate. This is in agreement with the XRD results of CFO powders. In light of the results of Figs. 4 and 6, the lowest annealing temperature of CFO films was chosen at 700 °C. The grain sizes of films prepared by the second sol–gel and then

**Table 4**

The grain sizes of films, prepared by the second sol–gel method and then annealed at different temperatures.

Annealing temperature (°C)	600	700
Grain size (nm)	51	62

annealed at two temperatures are shown in Table 4. It is seen that the grain sizes increase with the increase of annealing temperatures.

Fig. 7 shows SEM images of surfaces of CFO films annealed at different temperatures. When CFO film is annealed at 400 °C, there are no obvious grains which can be seen. When annealing temperature of CFO film is 500 °C or above, grains can be seen. With the increase of annealing temperature, the density and grain size of CFO film are increased. When annealed at 700 °C, the CFO film is crack-free and has compact structure without any pore. The grain size of CFO film is about 50 nm. When annealed at 750 °C, there are obvious

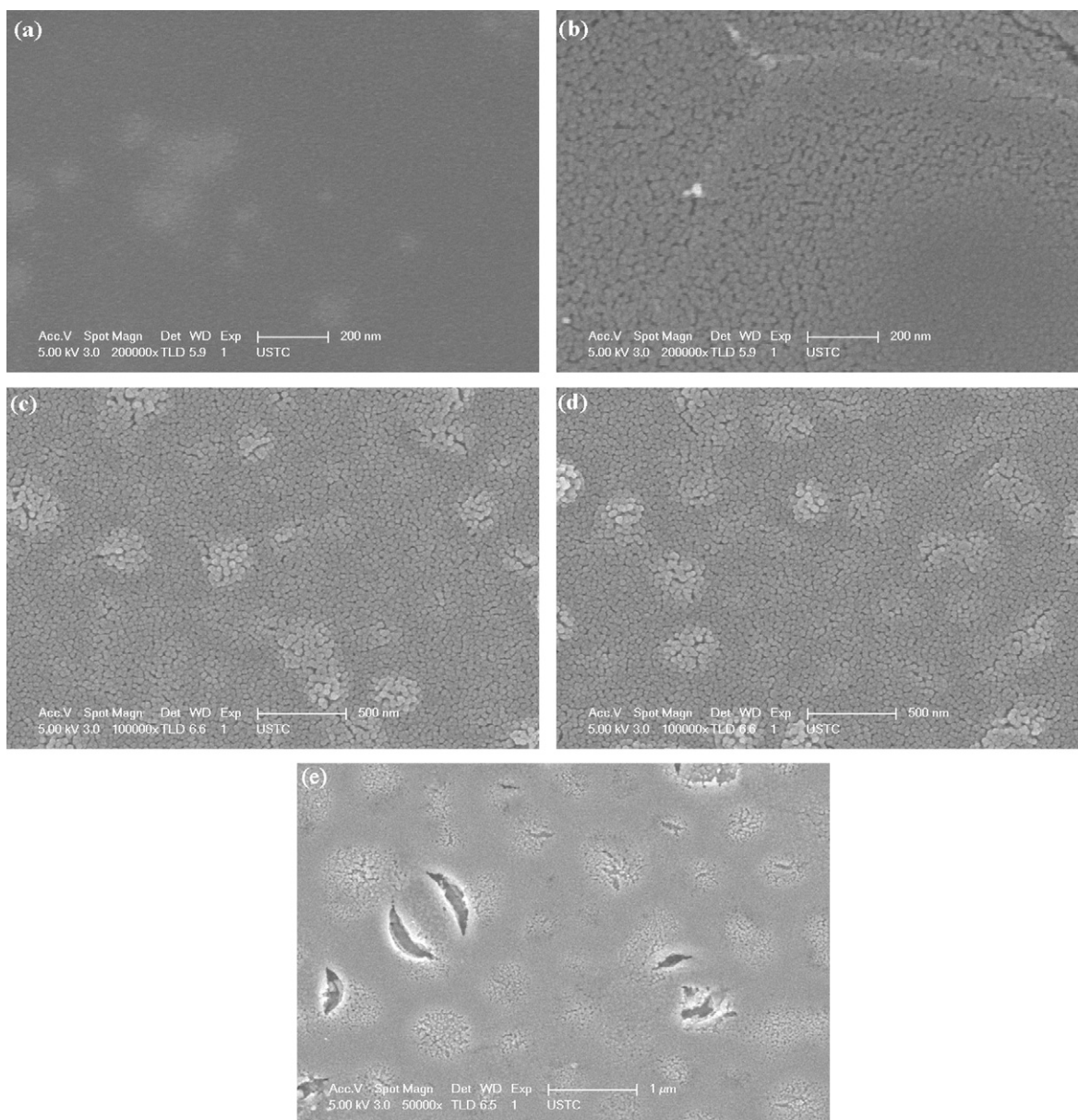


**Fig. 7.** SEM images of surface of CFO films synthesized by the second sol–gel annealed at different temperatures for 10 min. (a) 400 °C; (b) 500 °C; (c) 600 °C; (d) 700 °C; and (e) 750 °C.

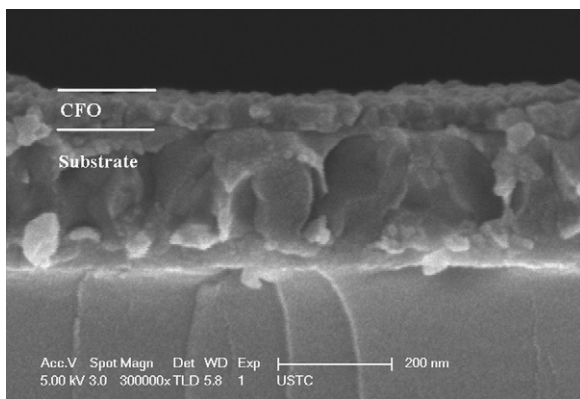


**Fig. 8.** SEM image of cross-section of CFO films synthesized by the second sol-gel annealed at 700 °C for 10 min (concentration of starting precursor solution is 0.15 mol L<sup>-1</sup>).

pores distributed unevenly in CFO films. This shows that the best annealing temperature of CFO films can be chose at 700 °C.

Fig. 8 shows SEM image of cross-section of CFO film annealed at 700 °C. It displays clear layered nanostructure. The average thickness of CFO film is about 49 nm. The surface of CFO film is relative flat.

In order to investigate the impact of the concentration of starting precursor solution on the morphologies of CFO film, the concentration was changed. Fig. 9 shows SEM image of cross-section of CFO film prepared by the second sol-gel method (concentration of the starting precursor solution is 0.30 mol L<sup>-1</sup>). It is seen that the surface of CFO film is bumpy and cross-sectional micrographs do not display the layered nanostructure when concentration of starting precursor solution is 0.30 mol L<sup>-1</sup>. This can be explained by the large stress in films during annealing process when the concentration of CFO starting precursor solution was high. For the surface of CFO film is much rougher and the film thickness in surface of CFO film is uneven, therefore the magnetic properties of CFO will be influenced. Compared with Fig. 8, it is clear that starting precursor solution with the concentration of 0.15 mol L<sup>-1</sup> is better for preparing CFO films with better morphologies.

From above results it can be concluded that the CFO films exhibit relatively better morphologies and the layered structure of films are more clearly visible compared with some other corresponding results. Except sol-gel process there are other methods used to prepare CFO films such as pulsed laser deposition (PLD).

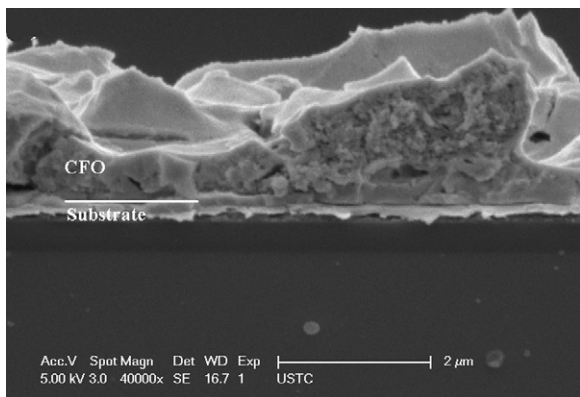


**Fig. 9.** SEM image of cross-section of CFO film synthesized by the second sol-gel annealed at 700 °C for 10 min (concentration of the starting precursor solution is 0.30 mol L<sup>-1</sup>).

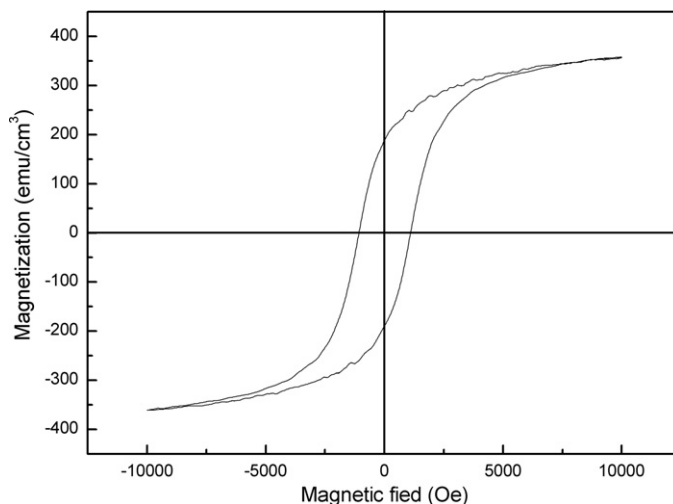


**Fig. 10.** Magnetic hysteresis loop of CFO film synthesized by the second sol-gel annealed at 700 °C for 10 min.

**Table 5**

The saturation magnetizations and coercivity of CFO films annealed at 700 °C.

Saturation magnetizations (emu/cm <sup>3</sup> )	coercivity (Oe)
358.45	1092.36

Single-crystal CFO films were prepared with much better morphologies by using PLD process, respectively [13]. But the PLD process is very expensive and not helpful to cost savings compared with sol-gel process.

Plots of magnetization (*M*) as a function of applied field (*H*) for CFO film prepared by the second sol-gel method are shown in Fig. 10. It is also seen that there exist a typical hysteresis loop. The saturation magnetizations and coercivities of CFO films are shown in Table 5. From Tables 3 and 5, it is seen that the coercivities of CFO films are greater than those of CFO powders. C.N. Chinnasamy [20] pointed that the relationship between *H<sub>c</sub>* (coercivity) and *d* (grain size) exhibited a maximum at 40 nm, corresponding to critical size of a single domain. When the grain sizes are greater than the critical size of a single domain, the coercivity is determined by magnetic displacement, so the value of coercivity is decreased with the increase of grain sizes. Comparing Table 2 with Table 4, it can be seen that the grain sizes of CFO films are smaller than that of CFO powders. Therefore the value of coercivity of CFO films is greater. In short, the CFO films have better magnetic properties than the CFO powders.

#### 4. Conclusions

The CFO starting precursor solutions were synthesized by two sol-gel methods. The CFO precursor solutions prepared by the second sol-gel method were spin-coated onto the Pt/Ti/SiO<sub>2</sub>/Si substrate in order to obtain CFO films. When annealed at 700 °C, CFO films are almost composed of the main phase and the substrate phase without secondary phases. With the increase of the annealing temperature, the density and grain size of CFO films and are increased. When annealed at 700 °C, the CFO film is crack-free and has compact structure without any pore. The thickness of CFO film is about 49 nm. The starting precursor solution with the concentration of 0.15 mol L<sup>-1</sup> is better for preparing CFO films than that with the concentration of 0.30 mol L<sup>-1</sup>. The CFO films have better magnetic properties than the CFO powders.

## Acknowledgement

Authors gratefully acknowledge the financial support from the Specialized Research Fund for the Doctoral Program of Higher Education (Grant No. 200803591037).

## References

- [1] B.H. Liu, J. Ding, Appl. Phys. Lett. 88 (2006) 42506–42513.
- [2] B.X. Gu, Z.H. Hua, J. Magn. Magn. Mater. 299 (2006) 392–396.
- [3] J.H. Yin, J. Ding, J.S. Chen, et al., J. Magn. Magn. Mater. 303 (2006) e387–e391.
- [4] F. Bodker, S. Morup, S. Linderoth, Phys. Rev. Lett. 72 (1994) 282–285.
- [5] M. Abe, T. Itoh, Y. Tamaura, Thin Solid Films 216 (1992) 155–161.
- [6] C.V. Gopal Reddy, S.V. Manorama, V.J. Rao, J. Mater. Sci. Lett. 19 (2000) 775–778.
- [7] S.D. Sartale, C.D. Lokhande, Ceram. Int. 28 (2002) 467–477.
- [8] J. Ding, Y.J. Chen, Y. Shi, et al., Appl. Phys. Lett. 77 (2000) 3621–3623.
- [9] J. Echigoaya, W. Asano, A. Yamaguchi, Phys. Status Solidi A 191 (2002) 359–369.
- [10] Y.C. Wang, J. Ding, J.B. Yi, et al., Appl. Phys. Lett. 84 (2004) 2596–2598.
- [11] H.Y. Zhang, B.X. Gu, H.R. Zhai, et al., Phys. Status Solidi A 143 (1994) 399–404.
- [12] S.N. Okuno, S. Hashimoto, K. Inomata, et al., J. Appl. Phys. 71 (1992) 5926–5929.
- [13] P.C. Dorsey, P. Lubitz, D.B. Chrisey, et al., J. Appl. Phys. 79 (1996) 6338–6340.
- [14] J.G. Lee, J.Y. Park, C.S. Kim, J. Mater. Sci. 33 (1998) 3965–3968.
- [15] S.G. Christoskova, M. Stoyanova, M. Georgieva, Appl. Catal. A: Gen. 208 (2001) 235–242.
- [16] C.O. Areán, M.P. Mentrui, E.E. Platero, et al., Mater. Lett. 39 (1999) 22–27.
- [17] Y. Cedeno-Mattei, O. Perales-Perez, Microelectron. J. 40 (2009) 673–676.
- [18] Y.Q. Qu, H.B. Yang, N. Yang, et al., Mater. Lett. 60 (2006) 3548–3552.
- [19] H.C. He, M.H. Ying, J.P. Zhou, et al., J. Electroceram. 21 (2008) 686–689.
- [20] C.N. Chinnsamy, B. Jeyadevan, K. Shinoda, et al., J. Appl. Phys. Lett. 83 (2003) 2862–2864.